Acta Crystallographica Section C
Crystal Structure Communications
ISSN 0108-2701
Editor: **Anthony Linden**

$Fe_{6.67}(PO_4)_{5.35}(HPO_4)_{0.65}$ and $Fe_{6.23}(PO_4)_{4.45}(HPO_4)_{1.55}$: two new mixed-valence iron phosphates

Fabrice Dal Bo and Frédéric Hatert

Acta Cryst. (2012). C**68**, i83–i85

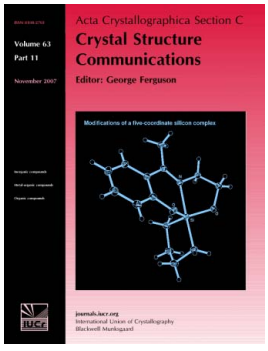

Acta Crystallographica Section C: Crystal Structure Communications specializes in the rapid dissemination of high-quality studies of crystal and molecular structures of interest in fields such as chemistry, biochemistry, mineralogy, pharmacology, physics and materials science. The numerical and text descriptions of each structure are submitted to the journal electronically as a Crystallographic Information File (CIF) and are checked and typeset automatically prior to peer review. The journal is well known for its high standards of structural reliability and presentation. *Section C* publishes approximately 1000 structures per year; readers have access to an archive that includes high-quality structural data for over 10000 compounds.

Acta Crystallographica Section C
Crystal Structure Communications
ISSN 0108-2701

$Fe_{6.67}(PO_4)_{5.35}(HPO_4)_{0.65}$ and $Fe_{6.23}(PO_4)_{4.45}(HPO_4)_{1.55}$: two new mixed-valence iron phosphates

Fabrice Dal Bo and Frédéric Hatert*

Laboratory of Mineralogy B.18, University of Liège, B-4000 Liège, Belgium
Correspondence e-mail: fhatert@ulg.ac.be

Received 27 July 2012
Accepted 15 October 2012
Online 29 November 2012

Two new mixed-valence iron phosphates, namely heptairon pentaphosphate hydrogen phosphate, $Fe_{6.67}(PO_4)_{5.35}(HPO_4)_{0.65}$, and heptairon tetraphosphate bis(hydrogen phosphate), $Fe_{6.23}(PO_4)_{4.45}(HPO_4)_{1.55}$, have been synthesized hydrothermally at 973 K and 0.1 GPa. The structures are similar to that of $Fe^{II}_3Fe^{III}_4(PO_4)_6$ and are characterized by infinite chains of Fe polyhedra parallel to the [101] direction. These chains are formed by the $Fe1O_6$ and $Fe2O_6$ octahedra, alternating with the $Fe4O_5$ distorted pentagonal bipyramids, according to the stacking sequence $\cdots$Fe1–Fe1–Fe4–Fe2–Fe2$\cdots$. The $Fe3O_6$ octahedra and PO_4 tetrahedra connect the chains together. Fe^{II} is localized on the Fe3 and Fe4 sites, whereas Fe^{III} is found in the Fe1 and Fe2 sites, according to bond-valence calculations. Refined site occupancies indicate the presence of vacancies on the Fe4 site, explained by the substitution mechanism $Fe^{II} + 2(PO_4^{3-})$ = vacancies + $2(HPO_4^{2-})$.

Comment

Only a few phosphates in nature contain iron in both valence states. The more common minerals with these chemical features are barbosalite–lipscombite $[Fe^{II}Fe^{III}_2(PO_4)_2(OH)_2]$, beraunite $[Fe^{II}Fe^{III}_5(PO_4)_4(OH)_5{\cdot}6H_2O]$, rockbridgeite $[Fe^{II}Fe^{III}_4(PO_4)_3(OH)_5]$ and whitmoreite $[Fe^{II}Fe^{III}_2(PO_4)_2(OH)_2{\cdot}4H_2O]$. They generally occur in granitic pegmatites as secondary minerals which are produced by the alteration of primary iron phosphates. Gorbunov *et al.* (1980) obtained the first synthetic iron phosphate with both Fe^{II} and Fe^{III}, with the formula $Fe^{II}_3Fe^{III}_4(PO_4)_6$. Redhammer *et al.* (2004) refined the structure of a similar compound containing a very small amount of sodium, $Na_{0.1}Fe_7(PO_4)_3$, and demonstrated that this phosphate was isotypic with the vanadate howerdevansite, $NaCu^{II}Fe^{III}_2(VO_4)_6$ (Hughes *et al.*, 1988). Lightfoot & Cheetham (1986) and Vencato *et al.* (1994) have shown that the reduction of Fe^{III} in $Fe^{II}_3Fe^{III}_4(PO_4)_6$ can induce the formation of isostructural hydrogen phosphates, with compositions $Fe^{II}_{7-x}Fe^{III}_x(PO_4)_{2+x}(PO_3OH)_{4-x}$ $(0 < x < 4)$.

In order to explore the stability of lithium iron phosphates, we decided to perform hydrothermal experiments in the Li–Fe^{II}–Fe^{III} (+PO_4) system, between 673 and 973 K, under a pressure of 0.1 GPa. In these experiments, various iron phosphates crystallized as, for example, $Fe_3(PO_4)_2$ (sarcopside-type), $Fe_7(PO_4)_6$, $Fe_3(PO_4)_2(OH)_2$ and $Fe_4(PO_4)_3(OH)_3$ (Dal Bo, 2011). $Fe_7(PO_4)_6$ is a stable phase between 673 and 973 K; electron-microprobe chemical analyses performed on 11 samples have shown variations of the Fe:P ratio from *ca* 7:6 to 6:6. In order to understand the variation of this ratio, single-crystal X-ray structural investigations were performed on two samples synthesized at 973 K (denoted H.339 and H.347).

The present paper reports the crystal structures of $Fe^{II}_{2.67}Fe^{III}_4(PO_4)_{5.35}(HPO_4)_{0.65}$ (H.339) and $Fe^{II}_{2.23}Fe^{III}_4(PO_4)_{4.45}(HPO_4)_{1.55}$ (H.347). Both structures were refined in the space group $P\overline{1}$ (No. 2) and are similar to those of corresponding iron phosphates and iron hydrogen phosphates reported in the literature (Redhammer *et al.*, 2004; Vencato *et al.*, 1994). The structures are characterized by isolated PO_4 tetrahedra and four different types of Fe polyhedra. Fe1, Fe2 and Fe3 occur in octahedral environments, whereas Fe4 occurs in a fivefold distorted trigonal bipyramid. Fe1, Fe2 and Fe4 are connected to each other by edge sharing to form infinite chains parallel to the [101] direction (Fig. 1). These chains are characterized by the stacking sequence $\cdots$Fe1–Fe1–Fe4–Fe2–Fe2$\cdots$, and the Fe3 octahedra connect the chains in the *b* direction by sharing corners with the Fe4 and Fe1 sites. As can be seen in Fig. 2, the PO_4 tetrahedra connect the chains together by corner sharing.

Refinement of the site-occupancy factors indicates that all Fe sites are fully occupied by iron, except for Fe4 which contains 0.8369 (18) and 0.614 (2) Fe^{II} in samples H.339 and H.347, respectively.

The charge deficit induced by this partial occupancy is compensated by the replacement of PO_4^{3-} by HPO_4^{2-}, according to the substitution mechanism $Fe^{II} + 2(PO_4^{3-})$ = vacancies + $2(HPO_4^{2-})$. Consequently, the general chemical formula of these phosphates can be expressed as $Fe^{II}_{1+2x}Fe^{III}_4(PO_4)_{4x+2}(HPO_4)_{4-4x}$, in which x = 0.84 (sample

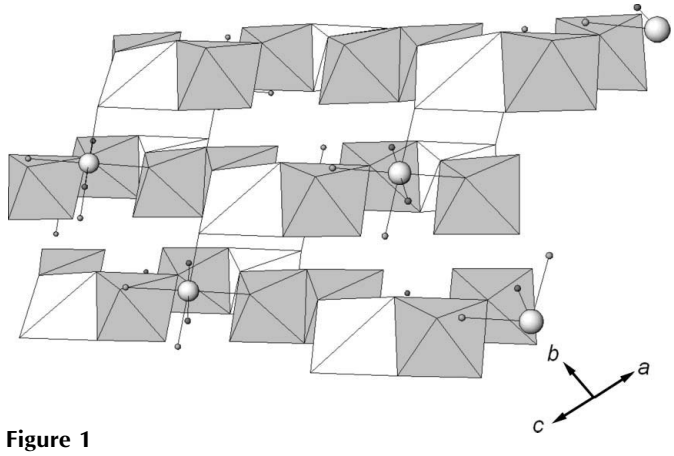

Figure 1
A representation of three infinite chains of Fe polyhedra. Key: $Fe1O_6$ and $Fe2O_6$ polyhedra are dark grey, $Fe4O_5$ polyhedra are white, Fe3 atoms are represented by white spheres and O atoms are represented by dark spheres.

 doi:10.1107/S0108270112043016

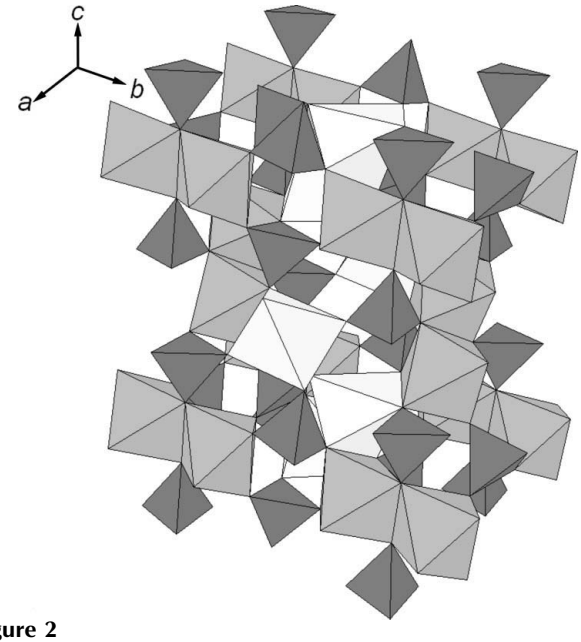

Figure 2
The crystal structure of $Fe^{II}_{2.67}Fe^{III}_{4}(PO_4)_{5.35}(HPO_4)_{0.65}$. Key: $Fe1O_6$ and $Fe2O_6$ polyhedra are dark grey, $Fe3O_6$ and $Fe4O_5$ polyhedra are light grey and PO_4 tetrahedra are dark.

H.339) or 0.61 (sample H.347). The substitution mechanism observed in the title compounds is completely different from that described by Lightfoot & Cheetham (1986) and Vencato *et al.* (1994), which corresponds to $Fe^{III} + PO_4^{3-} = Fe^{II} + HPO_4^{2-}$. In this last case, the charge deficit is produced by reducing Fe^{III} into Fe^{II}, whereas in samples H.339 and H.347 this deficit is produced by the appearance of vacancies on the Fe4 five-coordinated site.

Since Li was present in the starting material used for the synthesis experiments, we decided to perform another refinement in which the Fe4 site is occupied simultaneously by Fe and Li. This refinement shows a site population of 0.44 Li + 0.56 Fe, but the bond-valence sum of 1.41, calculated from the Fe4—O bond lengths, is in poor agreement with the expected value of 1.56. In the final refinement cycle, we consequently adopted the most realistic model, in which the Fe4 site is occupied by Fe^{II} and vacancies, without any significant amount of lithium.

The final site populations, calculated from the observed site occupancies and assuming charge balance, are Fe^{III} on the Fe1 and Fe2 sites, Fe^{II} on the Fe3 site, and Fe^{II} plus vacancies on the Fe4 site. Bond-valence sums, calculated by using the empirical parameters of Brown & Altermatt (1985), confirm the distributions of Fe^{II} and Fe^{III} among the different crystallographic sites. Indeed, the Fe1, Fe2, Fe3 and Fe4 bond-valence sums are 3.01, 3.07, 1.82 and 1.96 (H.339) or 3.09, 3.10, 2.07 and 1.94 (H.347), respectively. The bond-valence sums for P1, P2 and P3 are 4.92, 4.95 and 5.04 (H.339), or 4.93, 4.96, 5.03 (H.347), respectively.

Experimental

Both single crystals used for the structure refinement were synthesized under hydrothermal conditions. The starting materials were prepared by mixing Li_3PO_4, $FePO_4$ and Fe in the molar proportions 1:5:1 (H.339) and 1:11.5:1 (H.347), and then homogenizing this mixture in an agate mortar. About 25 mg of each mixture were sealed in gold tubes with outer diameters of 2 mm and lengths of 25 mm, containing 2 mg of pure water. The gold capsules were then inserted in a Tuttle-type pressure vessel (Tuttle, 1949) and maintained at a temperature of 973 K and a pressure of 0.1 GPa. After 7 d, the gold tubes containing the samples were quenched in the autoclave to room temperature in a stream of cold air. Black crystals of H.339 were found in association with colourless crystals of $LiFePO_4$ and green crystals of $Li_3Fe_2(PO_4)_3$. Black crystals of H.347 crystallized in association with light-green crystals of $LiFe(P_2O_7)$ and $Li_3Fe_2(PO_4)_3$.

A chemical analysis has been performed with a CAMEBAX SX-100 electron microprobe (15 kV acceleration voltage, 5 nA beam current). The standard used to calibrate both Fe and P was graftonite from Kabira (sample KF16, Fransolet, 1975). The average of ten point analyses for H.339 gives P_2O_5 44.90, FeO* 20.00, Fe_2O_3* 33.68, H_2O* 0.68, *i.e.* total 99.27 wt% [* indicates values calculated to maintain charge balance, assuming the substitution mechanism $Fe^{II} + 2(PO_4^{3-})$ = vacancies + $2(HPO_4^{2-})$]. The chemical composition, calculated on the basis of six P atoms and four Fe^{III} atoms per formula unit, corresponds to $Fe^{II}_{2.64}Fe^{III}_{4}(PO_4)_{5.28}(HPO_4)_{0.72}$. For H.347, the average of 12 point analyses gives P_2O_5 46.57, FeO* 15.11, Fe_2O_3* 34.93, H_2O* 1.80, *i.e.* total 99.68 wt%. The chemical composition, calculated on the basis of six P atoms and four Fe^{III} atoms per formula unit, corresponds to $Fe^{II}_{2.08}Fe^{III}_{4}(PO_4)_{4.16}(HPO_4)_{1.84}$. Both formulas are in fairly good agreement with the compositions calculated from the structural data, which are $Fe^{II}_{2.67}Fe^{III}_{4}(PO_4)_{5.35}(HPO_4)_{0.65}$ (H.339) and $Fe^{II}_{2.23}Fe^{III}_{4}(PO_4)_{4.45}(HPO_4)_{1.55}$ (H.347).

Sample H.339

Crystal data

$Fe_{6.67}(PO_4)_{5.35}(HPO_4)_{0.65}$
M_r = 942.93
Triclinic, $P\overline{1}$
a = 6.3609 (10) Å
b = 7.9750 (13) Å
c = 9.3220 (15) Å
α = 105.278 (14)°
β = 108.055 (14)°
γ = 101.993 (14)°
V = 411.55 (12) Å^3
Z = 1
Mo $K\alpha$ radiation
μ = 6.44 mm^{-1}
T = 293 K
0.10 × 0.08 × 0.07 mm

Data collection

Agilent Xcalibur Eos diffractometer
Absorption correction: multi-scan (*CrysAlis PRO*; Agilent, 2012)
T_{min} = 0.543, T_{max} = 0.640
21890 measured reflections
2404 independent reflections
2084 reflections with $I > 2\sigma(I)$
R_{int} = 0.039

Refinement

$R[F^2 > 2\sigma(F^2)]$ = 0.024
$wR(F^2)$ = 0.057
S = 1.10
2404 reflections
170 parameters
$\Delta\rho_{max}$ = 0.62 e Å^{-3}
$\Delta\rho_{min}$ = −0.50 e Å^{-3}

Sample H.347

Crystal data

$Fe_{6.23}(PO_4)_{4.45}(HPO_4)_{1.55}$
M_r = 919.26
Triclinic, $P\overline{1}$
a = 6.3445 (2) Å
b = 7.9353 (3) Å
c = 9.2829 (3) Å
α = 105.303 (3)°
β = 108.176 (3)°
γ = 101.700 (3)°
V = 407.03 (2) Å^3
Z = 1
Mo $K\alpha$ radiation
μ = 6.13 mm^{-1}
T = 293 K
0.15 × 0.10 × 0.06 mm

Data collection

Agilent Xcalibur Eos diffractometer
Absorption correction: analytical [*CrysAlis PRO* (Agilent, 2012), based on expressions derived by Clark & Reid (1995)]
T_{min} = 0.573, T_{max} = 0.786
21571 measured reflections
2378 independent reflections
2167 reflections with $I > 2\sigma(I)$
R_{int} = 0.031

Refinement

$R[F^2 > 2\sigma(F^2)]$ = 0.027
$wR(F^2)$ = 0.085
S = 1.13
2378 reflections
174 parameters
H atoms treated by a mixture of independent and constrained refinement
$\Delta\rho_{max}$ = 0.96 e Å^{-3}
$\Delta\rho_{min}$ = −0.67 e Å^{-3}

All atoms were refined anisotropically in both structures. The refined site-occupancy factors then indicated low electronic densities on the Fe4 site, thus showing that this site was not fully occupied by Fe^{II}. Therefore, Fe^{II} and vacancies were refined on the Fe4 site. The low amounts of HPO_4^{2-} groups occurring in sample H.339 prevented any determination of H-atom positions; however, one H-atom position was located in sample H.347 by a difference Fourier map.

For both compounds, data collection: *CrysAlis PRO* (Agilent, 2012); cell refinement: *CrysAlis PRO*; data reduction: *CrysAlis PRO*; program(s) used to solve structure: *SHELXS97* (Sheldrick, 2008); program(s) used to refine structure: *SHELXL97* (Sheldrick, 2008); molecular graphics: *ATOMS* (Dowty, 1993); software used to prepare material for publication: *OLEX2* (Dolomanov *et al.*, 2009).

The authors thank Dr Simon Philippo (National History Museum of Luxembourg) for his financial support in the realization of a PhD thesis, and analyst T. Theye, Stuttgart, Germany, for help with the electron-microprobe analyses. FH thanks the FNRS (Belgium) for the position of 'Chercheur qualifié', and for grant Nos. 1.5.113.05.F and 1.5.098.06.F.

Supplementary data for this paper are available from the IUCr electronic archives (Reference: FN3113). Services for accessing these data are described at the back of the journal.

References

Agilent (2012). *CrysAlis PRO*. Agilent Technologies, Yarnton, Oxfordshire, England.
Brown, I. D. & Altermatt, D. (1985). *Acta Cryst.* B**41**, 244–247.
Clark, R. C. & Reid, J. S. (1995). *Acta Cryst.* A**51**, 887–897.
Dal Bo, F. (2011). Unpublished Masters thesis, University of Liège, Belgium.
Dolomanov, O. V., Bourhis, L. J., Gildea, R. J., Howard, J. A. K. & Puschmann, H. (2009). *J. Appl. Cryst.* **42**, 339–341.
Dowty, E. (1993). *ATOMS for Windows*. Shape Software, Kingsport, Tennessee, USA.
Fransolet, A.-M. (1975). Unpublished PhD thesis, University of Liège, Belgium.
Gorbunov, Y. A., Maksimov, B. A., Kabalov, Y. K., Ivashenko, A. N., Mel'nikov, O. K. & Belov, N. V. (1980). *Dokl. Akad. Nauk SSSR*, **254**, 873.
Hughes, J. M., Drexler, J. W., Campana, C. F. & Malinconico, M. L. (1988). *Am. Mineral.* **73**, 181–186.
Lightfoot, P. & Cheetham, A. K. (1986). 3rd European Conference on Solid State Chemistry, Regensburg. Abstracts, Vol. 2, p. 410.
Redhammer, G. J., Roth, G., Tippelt, G., Bernroider, M., Lottermoser, W. & Amthauer, G. (2004). *J. Solid State Chem.* **177**, 1607–1618.
Sheldrick, G. M. (2008). *Acta Cryst.* A**64**, 112–122.
Tuttle, O. F. (1949). *Geol. Soc. Am. Bull.* **60**, 1727–1729.
Vencato, I., Moreira, L. F., Mattievich, E. & Mascarenhas, Y. P. (1994). *J. Braz. Chem. Soc.* **5**, 43–51.

supplementary materials

Acta Cryst. (2012). C**68**, i83–i85 [doi:10.1107/S0108270112043016]

$Fe_{6.67}(PO_4)_{5.35}(HPO_4)_{0.65}$ and $Fe_{6.23}(PO_4)_{4.45}(HPO_4)_{1.55}$: two new mixed-valence iron phosphates

Fabrice Dal Bo and Frédéric Hatert

(H339) Heptairon pentaphosphate hydrogen phosphate

Crystal data

$Fe_{6.67}(PO_4)_{5.35}(HPO_4)_{0.65}$
$M_r = 942.93$
Triclinic, $P\overline{1}$
$a = 6.3609$ (10) Å
$b = 7.9750$ (13) Å
$c = 9.3220$ (15) Å
$\alpha = 105.278$ (14)°
$\beta = 108.055$ (14)°
$\gamma = 101.993$ (14)°
$V = 411.55$ (12) Å^3
$Z = 1$
$F(000) = 456.07$
$D_x = 3.804$ Mg m^{-3}
Mo $K\alpha$ radiation, $\lambda = 0.7107$ Å
Cell parameters from 7440 reflections
$\theta = 2.5$–30.4°
$\mu = 6.44$ mm^{-1}
$T = 293$ K
Isometric crystal, black
0.10 × 0.08 × 0.07 mm

Data collection

Agilent Xcalibur Eos diffractometer
Radiation source: Enhance (Mo) X-ray Source
Graphite monochromator
Detector resolution: 16.0087 pixels mm^{-1}
ω scans
Absorption correction: multi-scan (*CrysAlis PRO*; Agilent, 2012)
$T_{min} = 0.543$, $T_{max} = 0.640$
21890 measured reflections
2404 independent reflections
2084 reflections with $I > 2\sigma(I)$
$R_{int} = 0.039$
$\theta_{max} = 30.5°$, $\theta_{min} = 2.5°$
$h = -9 \rightarrow 8$
$k = -11 \rightarrow 11$
$l = -13 \rightarrow 13$

Refinement

Refinement on F^2
Least-squares matrix: full
$R[F^2 > 2\sigma(F^2)] = 0.024$
$wR(F^2) = 0.057$
$S = 1.10$
2404 reflections
170 parameters
0 restraints
Primary atom site location: structure-invariant direct methods
Secondary atom site location: difference Fourier map
$w = 1/[\sigma^2(F_o^2) + (0.0224P)^2 + 0.4764P]$ where $P = (F_o^2 + 2F_c^2)/3$
$(\Delta/\sigma)_{max} < 0.001$
$\Delta\rho_{max} = 0.62$ e Å^{-3}
$\Delta\rho_{min} = -0.50$ e Å^{-3}

Special details

Experimental. Absorption correction: CrysAlisPro, Agilent Technologies, Version 1.171.35.21 (release 20-01-2012 CrysAlis171 .NET) (compiled Jan 23 2012,18:06:46) Empirical absorption correction using spherical harmonics, implemented in SCALE3 ABSPACK scaling algorithm.

Geometry. All esds (except the esd in the dihedral angle between two l.s. planes) are estimated using the full covariance matrix. The cell esds are taken into account individually in the estimation of esds in distances, angles and torsion angles; correlations between esds in cell parameters are only used when they are defined by crystal symmetry. An approximate (isotropic) treatment of cell esds is used for estimating esds involving l.s. planes.

Refinement. Refinement of F^2 against ALL reflections. The weighted R-factor wR and goodness of fit S are based on F^2, conventional R-factors R are based on F, with F set to zero for negative F^2. The threshold expression of $F^2 > 2\text{sigma}(F^2)$ is used only for calculating R-factors(gt) etc. and is not relevant to the choice of reflections for refinement. R-factors based on F^2 are statistically about twice as large as those based on F, and R- factors based on ALL data will be even larger.

Fractional atomic coordinates and isotropic or equivalent isotropic displacement parameters (Å²)

	x	*y*	*z*	U_{iso}*/U_{eq}	Occ. (<1)
Fe1	0.11782 (6)	0.04568 (5)	0.38554 (4)	0.01338 (8)	
Fe2	0.45486 (6)	−0.22200 (5)	−0.02741 (4)	0.01292 (9)	
Fe3	0.5000	0.5000	0.5000	0.01590 (11)	
Fe4	0.21811 (7)	−0.31143 (6)	0.21270 (5)	0.01511 (14)	0.8369 (18)
P1	0.40324 (10)	−0.09557 (8)	0.66575 (7)	0.01167 (12)	
P2	−0.27138 (10)	−0.34924 (8)	0.26723 (7)	0.01186 (12)	
P3	−0.09965 (11)	−0.26775 (9)	−0.12952 (7)	0.01258 (12)	
O1	0.1896 (3)	−0.0383 (2)	0.5847 (2)	0.0139 (3)	
O2	−0.0426 (3)	−0.2318 (2)	0.2725 (2)	0.0141 (3)	
O3	0.5193 (3)	−0.3106 (2)	0.1581 (2)	0.0146 (3)	
O4	0.1344 (3)	−0.2605 (2)	−0.0070 (2)	0.0156 (3)	
O5	0.3790 (3)	−0.0296 (2)	0.3387 (2)	0.0152 (3)	
O6	0.4322 (3)	−0.0519 (2)	−0.1545 (2)	0.0137 (3)	
O7	−0.2224 (3)	−0.4589 (2)	−0.2611 (2)	0.0183 (4)	
O8	0.3704 (3)	−0.2918 (2)	0.5788 (2)	0.0196 (4)	
O9	0.7502 (3)	−0.2188 (3)	−0.0368 (2)	0.0192 (4)	
O10	−0.2888 (3)	−0.5483 (2)	0.2046 (2)	0.0172 (4)	
O11	0.0503 (3)	0.1327 (3)	0.2131 (2)	0.0191 (4)	
O12	0.2714 (3)	0.3008 (2)	0.5591 (2)	0.0150 (3)	

Atomic displacement parameters (Å²)

	U^{11}	U^{22}	U^{33}	U^{12}	U^{13}	U^{23}
Fe1	0.01316 (17)	0.01413 (17)	0.01370 (17)	0.00410 (13)	0.00582 (13)	0.00559 (13)
Fe2	0.01292 (16)	0.01290 (17)	0.01293 (17)	0.00412 (13)	0.00486 (13)	0.00465 (13)
Fe3	0.0193 (3)	0.0140 (2)	0.0158 (2)	0.00621 (19)	0.0078 (2)	0.0052 (2)
Fe4	0.0158 (2)	0.0144 (2)	0.0175 (2)	0.00576 (16)	0.00831 (17)	0.00637 (17)
P1	0.0118 (3)	0.0121 (3)	0.0117 (3)	0.0040 (2)	0.0051 (2)	0.0043 (2)
P2	0.0113 (3)	0.0122 (3)	0.0120 (3)	0.0034 (2)	0.0047 (2)	0.0041 (2)
P3	0.0115 (3)	0.0135 (3)	0.0127 (3)	0.0041 (2)	0.0046 (2)	0.0046 (2)
O1	0.0130 (8)	0.0161 (8)	0.0137 (8)	0.0053 (7)	0.0055 (6)	0.0057 (7)
O2	0.0125 (8)	0.0146 (8)	0.0152 (8)	0.0030 (6)	0.0065 (7)	0.0049 (7)
O3	0.0124 (8)	0.0165 (8)	0.0143 (8)	0.0041 (7)	0.0043 (6)	0.0059 (7)
O4	0.0138 (8)	0.0202 (9)	0.0140 (8)	0.0072 (7)	0.0054 (7)	0.0064 (7)
O5	0.0136 (8)	0.0172 (9)	0.0151 (8)	0.0035 (7)	0.0068 (7)	0.0056 (7)
O6	0.0150 (8)	0.0152 (8)	0.0125 (8)	0.0052 (7)	0.0060 (6)	0.0059 (7)
O7	0.0191 (9)	0.0148 (9)	0.0164 (9)	0.0048 (7)	0.0031 (7)	0.0031 (7)
O8	0.0258 (10)	0.0152 (9)	0.0197 (9)	0.0095 (8)	0.0100 (8)	0.0052 (7)

O9	0.0156 (8)	0.0281 (10)	0.0175 (9)	0.0098 (7)	0.0086 (7)	0.0084 (8)
O10	0.0181 (9)	0.0144 (8)	0.0176 (9)	0.0047 (7)	0.0066 (7)	0.0040 (7)
O11	0.0186 (9)	0.0194 (9)	0.0210 (9)	0.0045 (7)	0.0070 (7)	0.0115 (8)
O12	0.0157 (8)	0.0151 (8)	0.0124 (8)	0.0020 (7)	0.0058 (7)	0.0040 (7)

Geometric parameters (Å, º)

Fe1—O1	2.0877 (17)	Fe4—O2	2.0712 (18)
Fe1—O1^{i}	2.0501 (17)	Fe4—O3	2.1284 (18)
Fe1—O2	2.0529 (18)	Fe4—O4	2.1198 (18)
Fe1—O5	2.0092 (18)	Fe4—O5	2.0941 (19)
Fe1—O11	1.8802 (18)	Fe4—O7^{iii}	2.0017 (19)
Fe1—O12	2.0423 (18)	P1—O1	1.5588 (18)
Fe2—O3	1.9955 (18)	P1—O6^{ix}	1.5611 (18)
Fe2—O4	2.0727 (18)	P1—O5^{vii}	1.5493 (18)
Fe2—O6	2.0215 (17)	P1—O8	1.4963 (19)
Fe2—O6^{ii}	2.1921 (18)	P2—O2	1.5368 (18)
Fe2—O9	1.9028 (18)	P2—O3^{x}	1.5490 (18)
Fe2—O10^{iii}	1.9290 (19)	P2—O12^{i}	1.5627 (18)
Fe3—O12	2.2222 (17)	P2—O10	1.5070 (19)
Fe3—O12^{iv}	2.2222 (17)	P3—O4	1.5495 (18)
Fe3—O7^{v}	2.2635 (18)	P3—O9^{x}	1.5170 (19)
Fe3—O7^{vi}	2.2635 (18)	P3—O11^{v}	1.5225 (19)
Fe3—O8^{vii}	2.0688 (18)	P3—O7	1.5377 (19)
Fe3—O8^{viii}	2.0688 (18)		
O1^{i}—Fe1—O1	82.49 (7)	O8^{viii}—Fe3—O12	93.32 (7)
O1^{i}—Fe1—O2	82.94 (7)	O8^{vii}—Fe3—O12	86.68 (7)
O2—Fe1—O1	79.79 (7)	O8^{viii}—Fe3—O12^{iv}	86.68 (7)
O5—Fe1—O1	90.53 (7)	O8^{viii}—Fe3—O7^{v}	81.40 (7)
O5—Fe1—O1^{i}	162.52 (7)	O8^{vii}—Fe3—O7^{v}	98.60 (7)
O5—Fe1—O2	80.05 (7)	O8^{viii}—Fe3—O7^{vi}	98.60 (7)
O5—Fe1—O12	105.50 (7)	O8^{vii}—Fe3—O7^{vi}	81.40 (7)
O11—Fe1—O1	176.80 (8)	O8^{vii}—Fe3—O8^{viii}	179.999 (1)
O11—Fe1—O1^{i}	95.73 (8)	O2—Fe4—O3	163.02 (7)
O11—Fe1—O2	102.68 (8)	O2—Fe4—O4	96.12 (7)
O11—Fe1—O5	91.90 (8)	O2—Fe4—O5	77.69 (7)
O11—Fe1—O12	94.46 (8)	O4—Fe4—O3	76.48 (7)
O12—Fe1—O1	82.88 (7)	O5—Fe4—O3	86.85 (7)
O12—Fe1—O1^{i}	89.59 (7)	O5—Fe4—O4	89.29 (7)
O12—Fe1—O2	161.87 (7)	O7^{iii}—Fe4—O2	106.40 (7)
O3—Fe2—O4	80.51 (7)	O7^{iii}—Fe4—O3	89.61 (7)
O3—Fe2—O6^{ii}	85.77 (7)	O7^{iii}—Fe4—O4	131.85 (7)
O3—Fe2—O6	160.98 (7)	O7^{iii}—Fe4—O5	136.39 (7)
O4—Fe2—O6^{ii}	87.28 (7)	O1—P1—O6^{ix}	105.76 (10)
O6—Fe2—O4	99.45 (7)	O5^{vii}—P1—O1	107.68 (10)
O6—Fe2—O6^{ii}	75.25 (7)	O5^{vii}—P1—O6^{ix}	108.29 (10)
O9—Fe2—O3	92.25 (8)	O8—P1—O1	111.23 (11)
O9—Fe2—O4	171.18 (8)	O8—P1—O6^{ix}	113.87 (10)
O9—Fe2—O6^{ii}	97.27 (8)	O8—P1—O5^{vii}	109.75 (11)

O9—Fe2—O6	89.04 (8)	O2—P2—O3^{x}	109.81 (10)
O9—Fe2—O10^{iii}	94.14 (8)	O2—P2—O12^{i}	109.72 (10)
O10^{iii}—Fe2—O3	100.35 (8)	O3^{x}—P2—O12^{i}	108.83 (10)
O10^{iii}—Fe2—O4	82.31 (8)	O10—P2—O2	108.78 (10)
O10^{iii}—Fe2—O6	98.48 (8)	O10—P2—O3^{x}	110.94 (10)
O10^{iii}—Fe2—O6^{ii}	166.84 (7)	O10—P2—O12^{i}	108.74 (10)
O12—Fe3—O12^{iv}	180.0	O9^{x}—P3—O4	107.65 (10)
O12—Fe3—O7^{v}	94.64 (7)	O9^{x}—P3—O11^{v}	111.43 (11)
O12^{iv}—Fe3—O7^{v}	85.36 (7)	O9^{x}—P3—O7	110.85 (11)
O12^{iv}—Fe3—O7^{vi}	94.64 (7)	O11^{v}—P3—O4	108.84 (11)
O12—Fe3—O7^{vi}	85.36 (7)	O11^{v}—P3—O7	107.18 (11)
O7^{v}—Fe3—O7^{vi}	180.00 (9)	O7—P3—O4	110.91 (10)
O8^{vii}—Fe3—O12^{iv}	93.32 (7)		

Symmetry codes: (i) $-x, -y, -z+1$; (ii) $-x+1, -y, -z$; (iii) $-x, -y-1, -z$; (iv) $-x+1, -y+1, -z+1$; (v) $-x, -y, -z$; (vi) $x+1, y+1, z+1$; (vii) $-x+1, -y, -z+1$; (viii) $x, y+1, z$; (ix) $x, y, z+1$; (x) $x-1, y, z$.

(H347) Heptairon tetraphosphate bis(hydrogen phosphate)

Crystal data

$Fe_{6.23}(PO_4)_{4.45}(HPO_4)_{1.55}$
$M_r = 919.26$
Triclinic, $P\overline{1}$
$a = 6.3445$ (2) Å
$b = 7.9353$ (3) Å
$c = 9.2829$ (3) Å
$\alpha = 105.303$ (3)°
$\beta = 108.176$ (3)°
$\gamma = 101.700$ (3)°
$V = 407.03$ (2) Å^3
$Z = 1$
$F(000) = 445.53$
$D_x = 3.750$ Mg m^{-3}
Mo $K\alpha$ radiation, $\lambda = 0.7107$ Å
Cell parameters from 11179 reflections
$\theta = 2.5$–30.4°
$\mu = 6.13$ mm^{-1}
$T = 293$ K
Isometric crystal, black
0.15 × 0.10 × 0.06 mm

Data collection

Agilent Xcalibur Eos diffractometer
Radiation source: Enhance (Mo) X-ray Source
Graphite monochromator
Detector resolution: 16.0087 pixels mm^{-1}
ω scans
Absorption correction: analytical [*CrysAlis PRO* (Agilent, 2012), based on expressions derived by Clark & Reid (1995)]
$T_{min} = 0.573$, $T_{max} = 0.786$
21571 measured reflections
2378 independent reflections
2167 reflections with $I > 2\sigma(I)$
$R_{int} = 0.031$
$\theta_{max} = 30.5°$, $\theta_{min} = 2.5°$
$h = -9\rightarrow9$
$k = -11\rightarrow11$
$l = -13\rightarrow13$

Refinement

Refinement on F^2
Least-squares matrix: full
$R[F^2 > 2\sigma(F^2)] = 0.027$
$wR(F^2) = 0.085$
$S = 1.14$
2378 reflections
170 parameters
0 restraints
Primary atom site location: structure-invariant direct methods
Secondary atom site location: difference Fourier map
Hydrogen site location: inferred from neighbouring sites
$w = 1/[\sigma^2(F_o^2) + (0.0503P)^2 + 0.6294P]$ where $P = (F_o^2 + 2F_c^2)/3$
$(\Delta/\sigma)_{max} < 0.001$
$\Delta\rho_{max} = 0.96$ e Å^{-3}
$\Delta\rho_{min} = -0.68$ e Å^{-3}

Special details

Experimental. Absorption correction: CrysAlisPro, Agilent Technologies, Version 1.171.35.21 (release 20-01-2012 CrysAlis171 .NET) (compiled Jan 23 2012,18:06:46) Analytical numeric absorption correction using a multifaceted crystal model based on expressions derived by R.C. Clark & J.S. Reid. (Clark, R. C. & Reid, J. S. (1995). Acta Cryst. A51, 887-897)

Geometry. All esds (except the esd in the dihedral angle between two l.s. planes) are estimated using the full covariance matrix. The cell esds are taken into account individually in the estimation of esds in distances, angles and torsion angles; correlations between esds in cell parameters are only used when they are defined by crystal symmetry. An approximate (isotropic) treatment of cell esds is used for estimating esds involving l.s. planes.

Refinement. Refinement of F^2 against ALL reflections. The weighted R-factor wR and goodness of fit S are based on F^2, conventional R-factors R are based on F, with F set to zero for negative F^2. The threshold expression of $F^2 > 2\text{sigma}(F^2)$ is used only for calculating R-factors(gt) etc. and is not relevant to the choice of reflections for refinement. R-factors based on F^2 are statistically about twice as large as those based on F, and R- factors based on ALL data will be even larger.

Fractional atomic coordinates and isotropic or equivalent isotropic displacement parameters (Å²)

	x	*y*	*z*	U_{iso}*/U_{eq}	Occ. (<1)
Fe1	−0.61697 (6)	0.45850 (5)	0.11678 (4)	0.00709 (11)	
Fe2	−0.04932 (6)	0.27698 (5)	0.47371 (5)	0.00698 (11)	
Fe3	1.0000	1.0000	0.0000	0.00897 (13)	
Fe4	0.28654 (11)	0.81443 (9)	0.28898 (8)	0.0096 (2)	0.614 (2)
P1	−0.09424 (11)	0.40554 (9)	0.16637 (8)	0.00517 (14)	
P2	0.77367 (11)	0.84989 (9)	0.23196 (8)	0.00504 (13)	
P3	−0.60279 (11)	0.23246 (9)	0.36786 (8)	0.00614 (14)	
O1	−0.3109 (3)	0.4594 (3)	0.0836 (2)	0.0071 (4)	
O2	0.1212 (3)	0.5322 (3)	0.1611 (2)	0.0084 (4)	
O3	0.5450 (3)	0.7327 (3)	0.2271 (2)	0.0081 (3)	
O4	−0.0673 (3)	0.4494 (3)	0.3459 (2)	0.0072 (3)	
O5	0.7909 (3)	1.0499 (3)	0.2929 (2)	0.0104 (4)	
O6	0.9837 (3)	0.8120 (3)	0.3417 (2)	0.0085 (4)	
O7	0.7306 (4)	0.9574 (3)	−0.2321 (3)	0.0145 (4)	
O8	−0.5490 (4)	0.3726 (3)	0.2886 (2)	0.0123 (4)	
O9	−0.3711 (3)	0.2344 (3)	0.4892 (2)	0.0103 (4)	
O10	0.2474 (3)	0.2797 (3)	0.4626 (2)	0.0118 (4)	
O11	0.7749 (3)	0.8007 (3)	0.0575 (2)	0.0081 (4)	
O12	0.8785 (4)	1.2081 (3)	0.0811 (3)	0.0139 (4)	

Atomic displacement parameters (Å²)

	U^{11}	U^{22}	U^{33}	U^{12}	U^{13}	U^{23}
Fe1	0.00555 (19)	0.0090 (2)	0.00715 (19)	0.00150 (14)	0.00292 (14)	0.00362 (15)
Fe2	0.00734 (18)	0.00644 (18)	0.00721 (19)	0.00230 (13)	0.00257 (14)	0.00266 (14)
Fe3	0.0105 (3)	0.0075 (2)	0.0098 (3)	0.00357 (19)	0.0047 (2)	0.0030 (2)
Fe4	0.0102 (3)	0.0091 (3)	0.0130 (4)	0.0046 (2)	0.0070 (2)	0.0048 (3)
P1	0.0052 (3)	0.0058 (3)	0.0052 (3)	0.0020 (2)	0.0025 (2)	0.0020 (2)
P2	0.0042 (3)	0.0054 (3)	0.0054 (3)	0.0013 (2)	0.0022 (2)	0.0015 (2)
P3	0.0053 (3)	0.0072 (3)	0.0072 (3)	0.0024 (2)	0.0030 (2)	0.0035 (2)
O1	0.0032 (8)	0.0112 (9)	0.0074 (8)	0.0023 (7)	0.0020 (6)	0.0042 (7)
O2	0.0071 (8)	0.0108 (9)	0.0090 (9)	0.0027 (7)	0.0048 (7)	0.0041 (7)
O3	0.0058 (8)	0.0092 (9)	0.0090 (8)	0.0010 (7)	0.0040 (7)	0.0023 (7)

O4	0.0091 (8)	0.0078 (8)	0.0058 (8)	0.0032 (7)	0.0034 (7)	0.0032 (7)
O5	0.0113 (9)	0.0075 (9)	0.0114 (9)	0.0033 (7)	0.0038 (7)	0.0021 (7)
O6	0.0055 (8)	0.0118 (9)	0.0089 (8)	0.0035 (7)	0.0023 (7)	0.0047 (7)
O7	0.0154 (10)	0.0076 (9)	0.0160 (10)	0.0009 (7)	0.0059 (8)	−0.0007 (8)
O8	0.0124 (9)	0.0135 (9)	0.0111 (9)	0.0018 (7)	0.0027 (7)	0.0086 (8)
O9	0.0062 (8)	0.0179 (10)	0.0110 (9)	0.0074 (7)	0.0038 (7)	0.0082 (8)
O10	0.0080 (9)	0.0203 (10)	0.0103 (9)	0.0075 (8)	0.0061 (7)	0.0048 (8)
O11	0.0092 (8)	0.0085 (9)	0.0057 (8)	0.0014 (7)	0.0038 (7)	0.0013 (7)
O12	0.0219 (10)	0.0086 (9)	0.0135 (10)	0.0065 (8)	0.0097 (8)	0.0028 (8)

Geometric parameters (Å, º)

Fe1—O1^{i}	2.0792 (19)	Fe4—O3	2.064 (2)
Fe1—O1	2.0576 (18)	Fe4—O6^{ii}	2.123 (2)
Fe1—O3^{ii}	2.025 (2)	Fe4—O2	2.096 (2)
Fe1—O2^{ii}	1.9910 (19)	Fe4—O9^{iv}	2.120 (2)
Fe1—O11^{iii}	2.0614 (19)	Fe4—O7^{viii}	2.029 (2)
Fe1—O8	1.8597 (19)	P2—O3	1.537 (2)
Fe2—O4	2.0314 (18)	P2—O5	1.506 (2)
Fe2—O4^{iv}	2.1731 (19)	P2—O6	1.5427 (19)
Fe2—O5^{v}	1.922 (2)	P2—O11	1.5652 (19)
Fe2—O6^{vi}	1.9805 (19)	P1—O1	1.5542 (19)
Fe2—O9	2.0573 (19)	P1—O4	1.5559 (19)
Fe2—O10	1.914 (2)	P1—O2	1.5462 (19)
Fe3—O11^{vii}	2.1979 (19)	P1—O12^{v}	1.504 (2)
Fe3—O11	2.1979 (19)	P3—O9	1.542 (2)
Fe3—O12	2.027 (2)	P3—O10^{ii}	1.519 (2)
Fe3—O12^{vii}	2.027 (2)	P3—O8	1.526 (2)
Fe3—O7^{vii}	2.182 (2)	P3—O7^{iii}	1.543 (2)
Fe3—O7	2.182 (2)		
O1—Fe1—O1^{i}	82.31 (8)	O12—Fe3—O7^{vii}	97.10 (8)
O1—Fe1—O11^{iii}	89.06 (8)	O12—Fe3—O7	82.90 (8)
O3^{ii}—Fe1—O1^{i}	79.82 (8)	O12^{vii}—Fe3—O7^{vii}	82.90 (8)
O3^{ii}—Fe1—O1	83.24 (8)	O7^{vii}—Fe3—O11	85.84 (7)
O3^{ii}—Fe1—O11^{iii}	161.92 (8)	O7—Fe3—O11	94.16 (7)
O2^{ii}—Fe1—O1	164.01 (8)	O7—Fe3—O11^{vii}	85.84 (7)
O2^{ii}—Fe1—O1^{i}	90.55 (8)	O7^{vii}—Fe3—O11^{vii}	94.16 (7)
O2^{ii}—Fe1—O3^{ii}	81.42 (8)	O7^{vii}—Fe3—O7	180.0
O2^{ii}—Fe1—O11^{iii}	104.31 (8)	O3—Fe4—O6^{ii}	162.47 (8)
O11^{iii}—Fe1—O1^{i}	82.96 (8)	O3—Fe4—O2	78.04 (8)
O8—Fe1—O1^{i}	176.45 (9)	O3—Fe4—O9^{iv}	96.77 (8)
O8—Fe1—O1	95.60 (8)	O2—Fe4—O6^{ii}	85.71 (8)
O8—Fe1—O3^{ii}	102.83 (8)	O2—Fe4—O9^{iv}	90.12 (8)
O8—Fe1—O2^{ii}	92.18 (9)	O9^{iv}—Fe4—O6^{ii}	76.56 (7)
O8—Fe1—O11^{iii}	94.16 (9)	O7^{viii}—Fe4—O3	107.08 (9)
O4—Fe2—O4^{iv}	74.85 (8)	O7^{viii}—Fe4—O6^{ii}	88.87 (8)
O4—Fe2—O9	100.32 (8)	O7^{viii}—Fe4—O2	133.66 (9)
O5^{v}—Fe2—O4^{iv}	167.77 (8)	O7^{viii}—Fe4—O9^{iv}	132.99 (9)
O5^{v}—Fe2—O4	97.53 (8)	O3—P2—O6	110.00 (11)

O5^{v}—Fe2—O6^{vi}	101.47 (8)	O3—P2—O11	110.02 (11)
O5^{v}—Fe2—O9	82.49 (9)	O5—P2—O3	109.10 (11)
O6^{vi}—Fe2—O4^{iv}	86.23 (8)	O5—P2—O6	110.91 (11)
O6^{vi}—Fe2—O4	160.96 (8)	O5—P2—O11	108.23 (11)
O6^{vi}—Fe2—O9	81.21 (8)	O6—P2—O11	108.56 (11)
O9—Fe2—O4^{iv}	89.40 (8)	O1—P1—O4	105.52 (11)
O10—Fe2—O4^{iv}	96.57 (8)	O2—P1—O1	107.80 (11)
O10—Fe2—O4	87.76 (8)	O2—P1—O4	108.80 (11)
O10—Fe2—O5^{v}	92.61 (9)	O12^{v}—P1—O1	111.44 (12)
O10—Fe2—O6^{vi}	92.45 (8)	O12^{v}—P1—O4	113.52 (11)
O10—Fe2—O9	171.01 (9)	O12^{v}—P1—O2	109.54 (12)
O11^{vii}—Fe3—O11	180.0	O9—P3—O7^{iii}	111.39 (12)
O12^{vii}—Fe3—O11^{vii}	94.28 (8)	O10^{ii}—P3—O9	107.21 (11)
O12—Fe3—O11^{vii}	85.72 (8)	O10^{ii}—P3—O8	111.87 (12)
O12^{vii}—Fe3—O11	85.72 (8)	O10^{ii}—P3—O7^{iii}	110.15 (12)
O12—Fe3—O11	94.28 (8)	O8—P3—O9	108.64 (11)
O12^{vii}—Fe3—O12	180.00 (10)	O8—P3—O7^{iii}	107.60 (12)
O12^{vii}—Fe3—O7	97.10 (8)		

Symmetry codes: (i) −*x*−1, −*y*+1, −*z*; (ii) *x*−1, *y*, *z*; (iii) −*x*, −*y*+1, −*z*; (iv) −*x*, −*y*+1, −*z*+1; (v) *x*−1, *y*−1, *z*; (vi) −*x*+1, −*y*+1, −*z*+1; (vii) −*x*+2, −*y*+2, −*z*; (viii) −*x*+1, −*y*+2, −*z*.